Tetrahedron Letters 51 (2010) 5680–5685

Contents lists available at ScienceDirect

Tetrahedron Letters

journal homepage: www.elsevier.com/locate/tetlet

Acridinedione-functionalized gold nanoparticles and model for the binding of 1,3-dithiol linked acridinedione on gold clusters

Ranganathan Velu, E. J. Padma Malar *,†, Vayalakkavoor T. Ramakrishnan, Perumal Ramamurthy *

National Centre for Ultrafast Processes, University of Madras, Taramani Campus, Chennai 600 113, India

ARTICLE INFO

Article history:
Received 6 June 2010
Revised 8 August 2010
Accepted 15 August 2010
Available online 19 August 2010

Keywords:
1,3-Dithiol ligands
Acridinedione
Fluorescence decay
1,2-Capping mode
Gold clusters

ABSTRACT

The design and synthesis of 1,3-dithiol linked acridinedione functionalized gold nanoparticles (**ADDDT-GNP**) is described. **ADDDT-GNP** was characterized by transmission electron microscopy (TEM), Fourier transform infrared (FT-IR), UV–vis, steady-state and time-resolved fluorescence techniques. Conformational analysis of 1,3-dithiol ligands using density functional theory (DFT) reveals that they can cap on gold clusters through 1,2-capping mode, in which the two sulfur atoms of the dithiol bind covalently with two adjacent gold atoms on the surface of the cluster. The present study shows that three conformers of the ligand can cap in the 1,2-mode of capping. The triexponential fluorescence decay observed in the capped nanogold complex with fluorophore-labeled 1,3-dithiol may originate from the three conformers of the complex in the 1,2-capping mode.

Metal nanoparticles play an important role in many different areas such as electronic, magnetic, catalysis, and biology.[1,2] They have also been widely exploited for their use in catalysis,[3] biological labeling,[4] photonic,[5] optoelectronic,[6] and information storage devices.[7] Various organic and biological sulfur-based compounds[8,9] are used to functionalize the gold nanoparticles. Mirkin and co-workers reported that the use of multithiolated species improves the stability of colloid gold nanoparticles.[10] The remarkable properties associated with nanoparticles can be rationalized, if the behavior of quantum-confined electrons in the nanometer scale is explored.[11,12] Gold nanoparticles are stabilized through capping with a wide variety of organic ligands such as amine, thiol,[8–10] dithiol, etc. A number of studies have investigated the nature of bonding between the nanometal and the ligand molecules.[13–21] The metal–ligand interactions in the organic-capping layer play a crucial role in the high performance materials.[22–25] In the recent years, several studies have been focused on the sulfur–gold bonding in alkanethiol self-assembled monolayers on Au(1 1 1).[23–33] However, the exact nature of the S–Au bond is still debated. In the case of dithiol ligands, it is found that gold nanoparticles are bound by both sulfur ends.[21]

In this work, we have synthesized the **ADDDT-GNP** (Scheme 1), with a fluorophore-labeled acridinedione derivative of 1,3-dithiol (**ADDDT**) and they were characterized. In order to understand the nature of bonding between the ligand sulfur atoms and the gold atoms in the capping layer, we have performed a simple modeling of the complex formation of 1,3-dithiol on gold cluster. We have examined in detail the different conformations of the simple 1,3-dithiol (1,3-dimercaptobutane) (**DTDMB**) and its molecular complex with gold atoms **Au-DTDMB** by density functional theory (DFT) calculations using B3LYP functionals.[33,34] We have also studied the conformations of **ADDDT**, and its gold complex **Au-ADDDT**. Based on the inferences of the conformational study, the capped complexes **Au-cap-DTDMB** are modeled using the ligand **DTDMB** in a cluster of eight Au atoms. The DFT predictions are corroborated with the experimental findings.

The synthesis of acridinedione disulfide (**ADDDS**), (precursor of **ADDDT**) and the **ADDDT-GNP**, were carried out as outlined in Scheme 1. Nitroacridinedione dye (**NADD**) was synthesized from tetraketone (**TK**) using the procedure reported in the literature.[35,36] Refluxing a mixture of **NADD** with Zn and $CaCl_2$ in ethanol yielded the aminoacridinedione **(AADD)**. An equimolar mixture of **AADD** and α-lipoic acid in dry dichloromethane in the presence of dicyclohexylcarbodiimide (DCC) on refluxing, afforded the **ADDDS**. Synthesis of gold nanoparticles functionalized with ADDDS was carried out by a modified procedure involving the biphase synthesis reported[15] by Brust et al. The details of the synthesis and characterization of acridinedione derivatives and its functionalized gold nanoparticles are given in the Supplementary data (Fig. S1 and S2).

The synthesized **ADDDT-GNP**, and **ADDDT**, were characterized by IR and ^{1}H NMR spectral studies. IR spectrum of the **ADDDT-GNP** showed no S–H stretching band. **ADDDT** showed the S–H

* Corresponding authors. Tel.: +91 44 24547190; fax: +91 44 24540709 (P.R.).
E-mail addresses: ejpmalar@yahoo.com (E.J. Padma Malar), prm60@hotmail.com (P. Ramamurthy).
† Address: Research Scientist C, University Grants Commission, New Delhi.

0040-4039/$ - see front matter © 2010 Elsevier Ltd. All rights reserved.
doi:10.1016/j.tetlet.2010.08.042

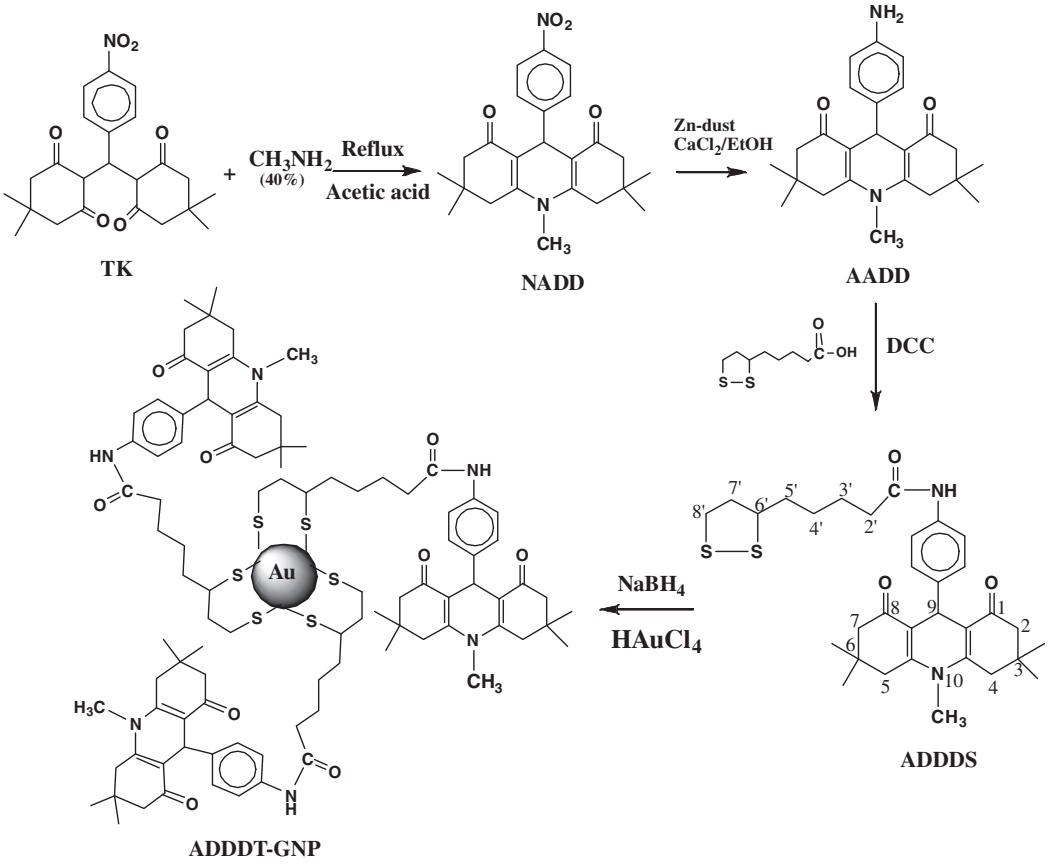

Scheme 1. Synthesis of **ADDDT-GNP**.

stretching vibration band at 2560 cm^{-1}. The computed S–H stretching frequencies for the dithiol comformers **ADDDT** a–f at B3LYP/6-31G* level are in the range of 2567–2581 cm^{-1} and are in good agreement with the experimental value of 2560 cm^{-1}. In the ^{1}H NMR study of the **ADDDT–GNP,** multiplicity of S–CH (C6′) and S-CH_2(C8′) are shifted towards up-field as compared with **ADDDS**. The IR and NMR spectral studies confirm S–Au bond formation in the **ADDDT-GNP**.[20]

The HR TEM image was recorded by drop-casting a dilute suspension of **ADDDT-GNP** on a carbon-coated copper grid and the images are presented in Figure 1. Three-dimensional approach in TEM images indicates that **ADDDT** is anchored on the surface of the gold nanoparticle (GNP). The GNP is found to have an average diameter of 2.5 nm and a total surface area of 19.625 nm^2.

The absorption and emission maxima of acridinedione dyes are centered around 380 and 430 nm, respectively.[35,36] The peak at 380 nm is attributed to the intramolecular charge transfer (ICT) from nitrogen to carbonyl oxygen in the acridinedione moiety, and the emission at 430 nm to that of the local excited (LE) state. Absorption spectrum of **ADDDS** is centered around 365 nm as shown in Figure S3 (see in Supplementary data) and the absorption spectrum of **ADDDT-GNP** (Fig. S3) consists of two bands: (i) the additive absorption spectrum of **ADDDS** due to ICT around 365 nm and (ii) a broad band in the visible region around

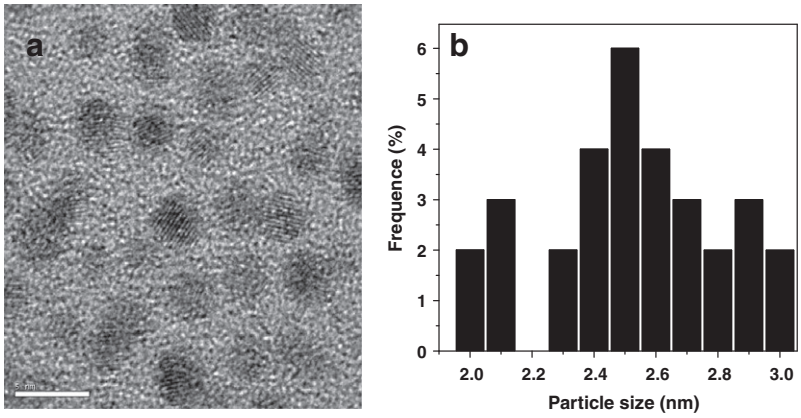

Figure 1. Typical HR-TEM image of **ADDDT-GNP**. (a) The size label is 5 nm. (b) Size-dependent histogram of **ADDDT-GNP**.

529 nm, which is attributed to the surface plasmon resonance (SPR) for the stabilized gold nanoparticles.

Fluorescence is an excellent probe for revealing the electronic characteristics of nanomaterials. In Figure S4, the emission spectra of free acridinedione and adsorbed species on gold nanoparticles taken in toluene are displayed. Free acridinedione exhibits a maximum emission peak around 440 nm, when excited at 365 nm. Similarly, the functionalized acridinedione on nanogold surface also exhibits a maximum emission at the same wavelength with a decrease in the fluorescence intensity as seen from Figure S4. The absorbance of acridinedione is the same in both cases. It is well-known that gold nanoparticles lead to quenching of fluorescence.[37–39] Drexhage et al. have observed a distance-dependent quenching of excited states of chromophores on metal surfaces.[40,41] Since metals in the nanoparticles are more electronegative than the bulk material, they can also participate in the electron transfer process.

The **ADDDS** and **ADDDT-GNP** have been investigated by the time-resolved fluorescence technique. Figure 2 presents the fluorescence decay of **ADDDS** and **ADDDT-GNP** monitored at 430 nm. The fluorescence decay of **ADDDS** in toluene exhibits triexponential behavior with lifetimes of 0.46, 1.0, and 3.0 ns with the amplitudes of 6.5%, 87% and 6.5%, respectively. The **ADDDT-GNP** also exhibits triexponential fluorescence decay with lifetimes of 0.7, 2.33 and 5.83 ns with amplitudes of 29%, 36% and 34%, respectively. The increase in the lifetime is attributed to the suppression of PET in **ADDDT-GNP** by nanogold. That is, electron transfer from the donor (–NH) moiety to the acceptor (nanogold). Increase in the lifetime of acridinedione derivatives was observed by suppression of PET in the interaction of acridinedione derivatives (–NH moiety) with metal (to form complexes) as reported by our group.[42,43] The observation of triexponential fluorescence decay reveals the presence of three major conformations in the **ADDDT-GNP**.

The two thiol groups in the 1,3-dithiol ligands **ADDDT** and **DTDMB** adopt different orientations leading to different conformations of the gold complexes **Au-ADDDT** and **Au-DTDMB**, respectively. The conformational features in the region of the thiol groups are similar in the corresponding conformers of **ADDDT** and **DTDMB**. The gold complexes **Au-DTDMB** and **Au-ADDDT** also exhibit similar orientations in the S–Au bonding regions. The different low-lying conformers of the gold complexes **Au-DTDMB** and **Au-ADDDT** are shown in Figures 3 and 4, respectively. It is seen that the relative stabilities of the conformers show the same trend at the different levels of the calculations performed (Table 1). Selected structural parameters in the gold complexes are shown in Table 2.

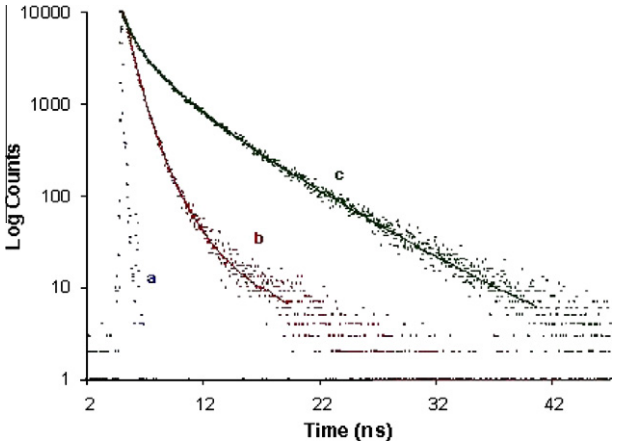

Figure 2. Fluorescence decay profile of **ADDDT**-capped nanogold in toluene; λ_{exc} = 375 nm and λ_{emi} = 480 nm: (a) laser profile; (b) **ADDDS** dye alone; (c) **ADDDT-GNP**.

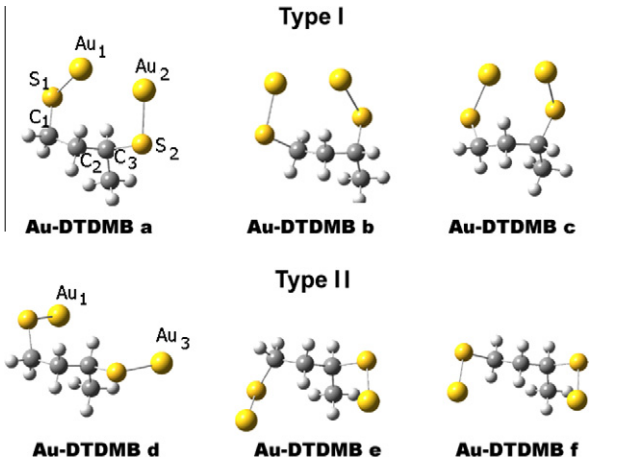

Figure 3. B3LYP optimized type I and type II conformers **Au-DTDMB** a–f. Ligand atoms were treated using 6-31G* basis set and the gold atoms were treated using LANL2DZ basis set. The labeling of atoms is shown.

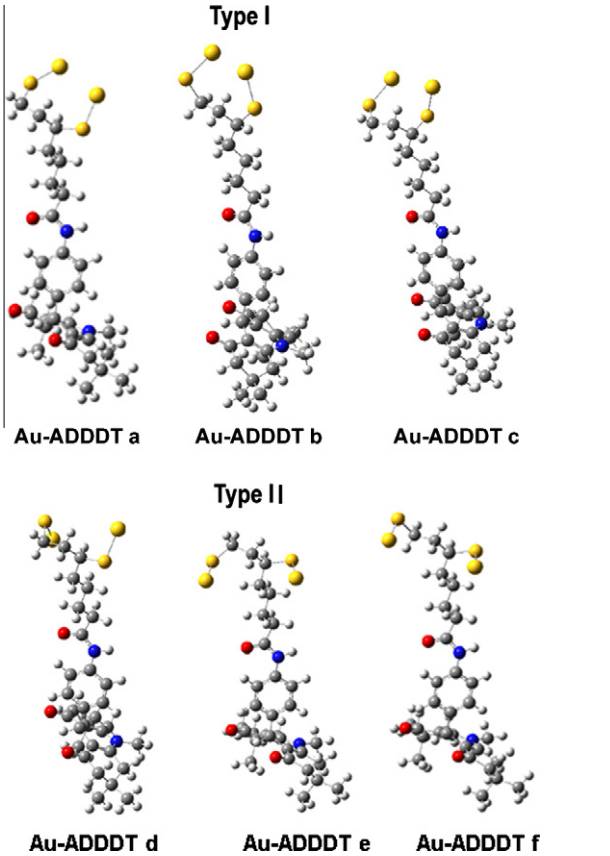

Figure 4. B3LYP optimized type I and type II conformers **Au-ADDDT** a–f. Ligand atoms were treated using 6-31G* basis set and the gold atoms were treated using LANL2DZ basis set.

The optimized geometries of the Au-dithiol complexes show that the Au-sulfur bond lengths are typical of single bond having covalent bond orders of about 1 (Table 2). Thus the Au–S lengths in complexes **Au-DTDMB** a–f and **Au-ADDDT** a–f are predicted in the range 2.31–2.34 Å and the covalent bond orders are found to vary from 0.9 to 1.0. This observation reveals that the gold–dithiol complexes are stabilized by the formation of covalent Au–S single bonds. Stability in the Au-alkanethiol monolayers is attributed to the formation of strong Au–S bond and the interactions among

Table 1
Total energies (in hartree) of the molecular gold complexes **Au-DTDMB** and **Au-ADDDT** and capped complexes **Au-cap-DTDMB** in the gold cluster

System[a]	B3LYP/6-31G*[b]	B3LYP/6-31+G*	B3LYP/6-31G* (toluene)/B3LYP/6-31G*
Au-DTDMB a	−1224.571890 (0.0)	−1224.581510 (0.0)	−1224.586744 (0.0)
Au-DTDMB b	−1224.571637 (0.2)	−1224.581248 (0.2)	−1224.586439 (0.2)
Au-DTDMB c	−1224.563019 (5.6)	−1224.571980 (6.0)	−1224.579349 (4.6)
Au-DTDMB d	−1224.563121 (5.5)	−1224.574627 (4.3)	−1224.581633 (3.2)
Au-DTDMB e	−1224.562504 (5.9)	−1224.573386 (5.1)	−1224.580990 (3.6)
Au-DTDMB f	−1224.565710 (3.9)	−1224.576744 (3.0)	−1224.584784 (1.2)
Au-ADDDT a	−2647.220394 (0.0)	−2647.277214 (0.0)	−2647.252362 (0.0)
Au-ADDDT b	−2647.218861 (1.0)	−2647.275420 (1.1)	−2647.251323 (0.7)
Au-ADDDT c	−2647.210303 (6.3)	−2647.266347 (6.8)	−2647.243895 (5.3)
Au-ADDDT d	−2647.211662 (5.5)	−2647.270118 (4.5)	−2647.246937 (3.4)
Au-ADDDT e	−2647.210881 (6.0)	−2647.268783 (5.3)	−2647.245791 (4.1)
Au-ADDDT f	−2647.214190 (3.9)	−2647.272328 (3.1)	−2647.249611 (1.7)
Au-cap-DTDMB a	—	−2037.420150	—
Au-cap-DTDMB b	—	−2037.415533	—
Au-cap-DTDMB c	—	−2037.405200	—

Relative energies in kcal/mol are given inside parentheses. The gold atoms are treated using LANL2DZ basis in all the conformers. Single point energy calculations were performed in the toluene medium and also in the cluster complexes **Au-cap-DTDMB**.

[a] Energy of gold atom in LANL2DZ basis-135.439785 hartree.

[b] In **Au-DTDMB** c the energy corresponds to single-point energy obtained using the structure optimized at B3LYP/6-31+G* level.

Table 2
Selected bond lengths in the gold complexes (in Å) using 6-31G* basis set for ligand atoms and LANL2DZ basis for gold atoms

Conformer	Au_1–S_1	Au_2–S_2/Au_3–S_2	$Au_1\cdots Au_2$/ $Au_1\cdots Au_3$	$S_1\cdots S_2$
Au-DTDMB a	2.332 (0.86)	2.337 (0.87)	2.921 (0.15)	4.725
Au-DTDMB b	2.338 (0.87)	2.329 (0.85)	2.916 (0.15)	4.709
Au-DTDMB c[a]	2.341 (0.90)	2.319 (0.96)	2.936 (0.19)	3.943
Au-DTDMB d	2.311 (0.97)	2.312 (0.97)	5.860	5.095
Au-DTDMB e	2.312(0.97)	2.315 (0.96)	5.731	5.409
Au-DTDMB f	2.312 (0.97)	2.314 (0.96)	5.860	5.626
Au-DTDMB g	2.308	2.311	8.330	4.910
Au-DTDMB h	2.313	2.311	6.450	4.990
Au-DTDMB i	2.316	2.325	7.465	3.115
Au-DTDMB j	2.313	2.311	7.332	4.526
Au-ADDDT a	2.332 (0.86)	2.336 (0.87)	2.920 (0.15)	4.711
Au-ADDDT b	2.335 (0.89)	2.337 (0.83)	2.876 (0.16)	4.867
Au-ADDDT c	2.343 (0.91)	2.325 (0.96)	2.933 (0.19)	3.893
Au-ADDDT d	2.312 (0.97)	2.310 (0.97)	6.084 (0.0)	5.116
Au-ADDDT e	2.312 (0.96)	2.314 (0.96)	6.109 (0.0)	5.399
Au-ADDDT f	2.312 (0.97)	2.315 (0.96)	5.963 (0.0)	5.613

The numbering of atoms follows the same order as in Figure 3. Covalent bond orders are inside parentheses.

[a] Structure optimized using 6-31+G* basis.

hydrocarbon chains.[23–27] Our study shows that the gold–sulfur bonding is covalent in origin.

The different structures of the gold complex **Au-DTDMB** (Fig. 3 and Table 2) reveal that they can be grouped into three types based on their Au···Au distances. In type I structures **Au-DTDMB** a–c the two gold atoms of the complex are separated by about 0.293 nm, which is close to the sum of atomic radii of the two gold atoms (radius = 0.144 nm). In type II structures **Au-DTDMB** d–f, the two gold atoms are separated by about 0.58 nm. Incidentally this distance is roughly four times the atomic radius of Au and smaller than the sum of van der Waals radii of four gold atoms (0.62 nm). In the structures **Au-DTDMB** g–j, the Au···Au distances are >0.64 nm. We have classified them as type III structures.

Analysis of the various conformations of the gold complex **Au-ADDDT**, also leads to the three types as seen in the case of system **Au-DTDMB** (Fig. 4 and Table 2). The Au···Au distances of 0.292, 0.288 and 0.293 nm, respectively, in **Au-ADDDT** a, **Au-ADDDT** b and **Au-ADDDT** c are very similar to the values predicted in **Au-DTDMB** a, **Au-DTDMB** b and **Au-DTDMB** c. The conformers **Au-ADDDT** d–f, have typical type II structures but the mean Au···Au distance is about 0.605 nm, which is on an average 0.02 nm longer than that observed in **Au-DTDMB** d–f. Overall conformational features in the two systems **Au-DTDMB** and **Au-ADDDT** are similar and are not influenced by the acridinedione substituent to any significant extent.

The low-lying conformations of the dithiol molecules remain the same till they interact with two isolated gold atoms or with two atoms on the surface of a cluster or with nanogold. Thus, the gold complex resulting from a suitable thiol conformer is expected to exhibit a similar structure in the molecular as well as the capped environments though some additional reorganization is expected to take place in the region of thiol groups in the capped complex. Since the capped gold atoms are in a uniform environment of other gold atoms on the surface, it is reasonable to assume that the geometries of the complexes in the two environments are comparable.

The structural analysis reveals that the two gold atoms are oriented away from the remaining part of the complex in the type I structures. From the distance of about 0.29 nm between the two gold atoms in the type I complexes, it may be inferred that they form the adjacent atoms on the surface of the gold cluster or nanogold. Thus, the complex structures **Au-DTDMB** a–c can be used to simulate the capped complexes involving S–Au bonding, without interference from the remaining part of the dithiol ligand. Since two neighboring gold atoms Au_1 and Au_2 on the surface of the cluster or nanogold interact and bind with the sulfur atoms of the dithiol, we refer it to as 1,2-capping mode (Fig. 5A and B). The separation of about 0.58 nm between the two gold atoms in the type II structures **Au-DTDMB** d–f leads to the inference such that in the corresponding capped structures another gold atom Au_2 can be placed in-between the capped gold atoms Au_1 and Au_3 in a linear arrangement (Fig. 5A and B). Since the capped gold atoms are alternate atoms on the surface we refer to the above as 1,3-capping mode. The orientations of gold atoms in the type III structures **Au-DTDMB** g–j are unsuitable to simulate the capped complexes

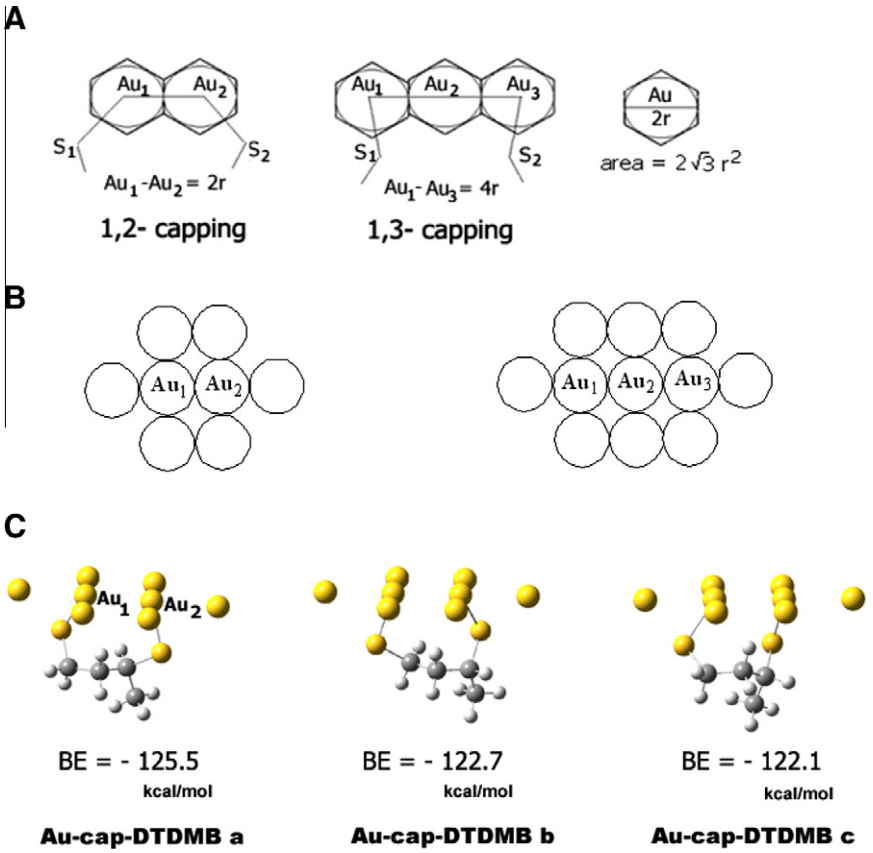

Figure 5. (A) Schematic illustration of 1,2-capping and 1,3-capping between dithiol and gold atoms. (B) The surface of the gold cluster used for modeling the two modes of capping. (C) Structures of 1,2-capped complex **Au-DTDMB** in gold cluster. Binding energies (in kcal/mol) of the capped complex in the gold cluster are shown.

as there is interference from the remaining part of the ligand. In the present work, we attempted to model the two modes of capping corresponding to the molecular complex structures **Au-DTDMB** a–f in a cluster of eight gold atoms.

Figure 5B depicts the model of the surface of gold cluster with the capped gold atoms labeled as Au_1 and Au_2 in the 1,2-mode of capping. We have modeled the 1,2-capped complexes of the gold cluster starting from the optimized type I conformers **Au-DTDMB** a–c, generated using 6-31+G* basis set on the ligand atoms. The resulting capped complexes **Au-cap-DTDMB** a–c (Fig. 5C) are subjected to single point computations at the same level. In **Au-cap-DTDMB** a–c the gold cluster is taken in a planar arrangement and the gold atoms adjacent to the capped gold atoms are at a distance of 0.293 nm (which is the mean Au···Au distance in **Au-DTDMB** a–c). The binding energy BE(x) in the capped complexes with Au_6 cluster surrounding the molecular complex is calculated as follows:

$$\mathrm{BE}(x) = E(\textbf{Au-cap-DTDMB}\ x) - [E(\textbf{Au-DTDMB}\ x) + 6E(\mathrm{Au})]$$

where x = a, b, c; E(**Au-cap-DTDMB** x) is the total energy of **Au-cap-DTDMB** x; E(**Au-DTDMB** x) is the total energy of **Au-DTDMB** x; E(Au) is the energy of gold atom at LANL2DZ level. It is seen that the molecular complex is stabilized significantly by 122–125 kcal/mol in the presence of the surrounding six gold atoms. Thus the present modeling study reveals the feasibility of 1,2-capping of two adjacent gold atoms on the surface of the cluster by 1,3-dithiol ligand. However, we could not model the 1,3-capped complexes in the gold cluster environment due to hindrance from a hydrogen atom of the second methylene group. The conclusion arrived above regarding the feasibility and stability of the three 1,2-capped complex structures **Au-cap-DTDMB** a–c in the gold cluster can indeed be extended to the nanogold system.

Structural information from experimental studies on nanometer-sized gold particles has been limited, due in part to the problem of preparing homogeneous material. X-ray structure determination of a *p*-mercaptobenzoic acid (*p*-MBA)-protected gold nanoparticle[30] showed 102 gold atoms and 44 *p*-MBAs. We have estimated that 265 gold atoms are present on the surface of nanogold of diameter 2.5 nm (Supplementary data), considering a hexagonally close packed model (Fig. 5A). The mean radius of 0.146 nm for the gold atom in the 1,2 capping mode (Fig. 5A), as predicted from the mean $Au_1 \cdots Au_2$ distance in conformers **Au-ADDDT** a–c, is used in the above computation. Number density of 13.89 atoms/nm^2 in the hexagonally closed packed nanogold surface[44] leads to 272 atoms, which shows that our theoretical model is quite reliable.

In summary, we have synthesized the **ADDDT-GNP**, and studied their photophysical properties. The conformational features of the ligand moieties and their gold complexes were examined using the DFT method. The present DFT modeling reveals that the 1,3-dithiol ligands form three conformers of capped complexes with gold cluster through 1,2-capping mode. The observation of tri-exponential fluorescence decay in the **ADDDT-GNP** reveals the presence of three conformers. The modeling study leads to the inference that the tri-exponential fluorescence decay in ADDDT-GNP originates from the three conformers of the 1,2-capped complex with **ADDDT**. The present results show that the gold–sulfur bonding in the molecular complexes of **ADDDT** with gold atoms is covalent in nature.

Acknowledgements

The authors are grateful to Professor K. Jug, Institut für Theoretische Chemie, Leibniz Universität Hannover, Germany for his interesting discussions and valuable suggestions. The computational

work was carried out using a generous grant of computational facility to EJPM at the Centre for Modeling Simulation and Design, University of Hyderabad, India.

Supplementary data

Supplementary data (detailed computational and synthetic procedures, characterization, ^{1}H and ^{13}C NMR data, FT-IR, HRMS, HR-TEM images and photophysical studies, experimental techniques, area of hexagonally close packed gold atom, estimation of number of gold atoms on the surface of the nanogold, and the cartesian coordinates of the various conformers) associated with this article can be found, in the online version, at doi:10.1016/j.tetlet.2010.08.042.

References and notes

1. Templeton, A. C.; Wuelfing, W. P.; Murray, R. W. *Acc. Chem. Res.* **2000**, *33*, 27.
2. El-Sayed, M. A. *Acc. Chem. Res.* **2001**, *34*, 257.
3. Lewis, L. N. *Chem. Rev.* **1993**, *93*, 2693.
4. Nicewarner-Pena, S. R. et al *Science* **2001**, *294*, 137.
5. Maier, S. A. et al *Adv. Mater.* **2001**, *13*, 1501.
6. Kamat, P. V. *J. Phys. Chem. B* **2002**, *106*, 7729.
7. Alivisatos, A. P. *Science* **1996**, *271*, 933.
8. Tshikhudo, T. R.; Demuru, D.; Wang, Z.; Brust, M.; Secchi, A.; Arduini, A.; Pochini, A. *Angew. Chem., Int. Ed.* **2005**, *44*, 2913.
9. Hasobe, T.; Imahori, H.; Kamat, P. V.; Ahn, T. K.; Kim, S. K.; Kim, D.; Fujimoto, A.; Hirakawa, T.; Fukuzumi, S. J. *Am. Chem. Soc.* **2005**, *127*, 1216.
10. Li, Z.; Jin, R.; Mirkin, C. A.; Letsinger, R. L. *Nucleic Acids Res.* **2002**, *30*, 1558.
11. *Nanoparticles: From Theory to Application*; Schmid, G., Ed.; Wiley-VCH: Weinheim, 2004.
12. *The Chemistry of Nanomaterials*; Rao, C. N. R., Muller, A., Cheetham, A. K., Eds.; Wiley-VCH: Weinheim, 2004.
13. Ding, Y.; Zhang, X.; Liu, X.; Guo, R. *Langmuir* **2006**, *22*, 2292.
14. Sainsbury, T.; Ikuno, T.; Okawa, D.; Pacile, D.; Frechet, J. M. J.; Zettl, A. *J. Phys. Chem. C* **2007**, *111*, 12992.
15. Brust, M.; Walker, M.; Bethell, D.; Schffrin, D. J.; Whyman, R. *J. Chem. Soc., Chem. Commun.* **1994**, 801.
16. He, S.; Yao, J.; Jiang, P.; Shi, D.; Zhang, H. *Langmuir* **2001**, *17*, 1571.
17. Ipe, B. I.; Yoosaf, K.; Thomas, K. G. *J. Am. Chem. Soc.* **2006**, *128*, 1907.
18. Yee, C.; Scotti, M.; Ulman, A.; White, H.; Rafailovich, M. S. J. *Langmuir* **1999**, *15*, 4314.
19. Kanehara, M.; Takahashi, H.; Teranishi, T. *Angew. Chem., Int. Ed.* **2008**, *46*, 307.
20. Zhao, Y. L.; Chen, Y.; Wang, M.; Lin, Y. *Org. Lett.* **2006**, *8*, 1267.
21. Garcia, B.; Salomé, M.; Lemelle, L.; Bridot, J.; Gillet, P.; Perriat, P.; Roux, S.; Tillement, O. *J. Chem. Soc., Chem. Commun.* **2005**, 369–371.
22. Russo, N. Metal–Ligand Interactions Moelcular-, Nano-, Micro-Systems in Complex Environments. In *NATO Science Series II Maths, Physics s publishing imprints*; Russo, N., Salahub, D. R., Witko, M., Eds.; Tec & Doc, Hermes Science Publications, Intercept, EM Inter, Synthèse agricole, 2003; Vol. 116,.
23. Schreiber, F. *J. Phys.: Condens. Matter* **2004**, *16*, R 881.
24. Schreiber, F. *Prog. Surf. Sci.* **2000**, *65*, 151.
25. Heimel, G.; Romaner, L.; Bredas, J. L.; Zojer, E. *Surf. Sci.* **2006**, *600*, 4548.
26. Vericat, C.; Vela, M. E.; Salvarezza, R. C. *Phys. Chem. Chem. Phys.* **2005**, *7*, 3258.
27. Vericat, C.; Vela, M. E.; Benitez, G. A.; Gago, J. A. M.; Torrelles, X.; Salvaezza, R. C. *J. Phys.: Condens. Matter* **2006**, *18*, 867.
28. Whetten, R. L.; Price, R. C. *Science* **2007**, *318*, 407.
29. Maksymovych, P.; Sorescu, D. C.; Yates, J. T. *J. Phys. Rev. Lett.* **2006**, *97*, 146103.
30. Jadzinsky, P. D.; Calero, G.; Ackerson, C. J.; Bushnell, D. A.; Kornberg, R. D. *Science* **2007**, *318*, 430.
31. Vericat, C.; Benitez, G. A.; Grumelli, D. E.; Vela, M. E.; Salvarezza, R. C. *J. Phys.: Condens. Matter.* **2008**, *20*, 184004.
32. Cossaro, A.; Mazzarello, R.; Rousseau, R.; Casalis, L.; Verdini, A.; Kohlmeyer, A.; Floreano, L.; Scandolo, S.; Morgante, A.; Klein, M. L.; Scoles, G. *Science* **2008**, *321*, 943.
33. Becke, A. D. *J. Chem. Phys.* **1993**, *98*, 5648.
34. Lee, C.; Yang, W.; Parr, R. G. *Phy. Rev. B* **1988**, *37*, 785.
35. Thiagarajan, V.; Ramamurthy, P.; Thirumalai, D.; Ramakrishnan, V. T. *Org. Lett.* **2005**, *7*, 657.
36. Srividya, N.; Ramamurthy, P.; Shanmugasundaram, P.; Ramakrishnan, V. T. *J. Org. Chem.* **1996**, *61*, 5083.
37. Lee, W. I.; Bae, Y.; Bard, A. *J. Am. Chem. Soc.* **2004**, *126*, 8358.
38. Oh, E.; Hong, M. Y.; Lee, D.; Nam, S. H.; Yoon, C. H.; Kim, H. S. *J. Am. Chem. Soc.* **2005**, *127*, 3270.
39. You, C. C.; De, M.; Han, G.; Retello, V. M. *J. Am. Chem. Soc.* **2005**, *127*, 12873.
40. Drexhage, K. H.; Kuhn, H.; Shafer, F. P.; Bunsen-Ges, B. *Phys. Chem.* **1968**, *72*, 329.
41. Drexhage, K. H.; Flock, M.; Kuhn, H.; Shafer, F. P.; Sperling, W.; Bunsen-Ges, B. *Phys. Chem.* **1969**, *73*, 1179.
42. Thiagarajan, V.; Selvaraju, C.; Padma Malar, E. J.; Ramamurthy, P. *Chem. Phys. Chem.* **2004**, *5*, 1200.
43. Ashokkumar, P.; Thiagarajan, V.; Vasanthi, S.; Ramamurthy, P. *J. Photochem. Photobiol., A* **2009**, *208*, 117.
44. Hostetler, M. J.; wingate, J. E.; Zhong, C. J.; Harris, J. E.; Vachet, R. W.; Clark, M. R.; Londono, J. D.; Green, S. J.; Stokes, J. *Langmuir* **1998**, *14*, 17.